Comput Mech (2005) 37: 24–31
DOI 10.1007/s00466-005-0694-1

ORIGINAL PAPER

A. Frangi · A. di. Gioia

Multipole BEM for the evaluation of damping forces on MEMS

Received: 25 May 2004 / Accepted: 29 December 2004 / Published online: 6 July 2005

Abstract A procedure for the analysis of 3D Stokes flow around complex micro structures (MEMS) is developed with the aim of evaluating damping forces. First kind integral equations employing single layer potentials are utilized and the linear system stemming from their discretization is solved by a GMRES iterative procedure with multipole accelerators. Issues pertaining to the conditioning of the linear system are discussed with reference to the examples presented.

1 Introduction

Micro-Electro-Mechanical-Systems (MEMS) are complex micro-structures employed as sensors or actuators in modern technologies. In this work the attention is focused on silicon MEMS where the actuation or sensing is performed electrostatically by means of arrays of capacitors. Such MEMS often consist of several substructures generally termed rotors and stators according to whether they are constrained to a substrate or free to translate/rotate. Especially at a first stage of the design and analysis steps this substructures can be simulated as rigid modules with concentrated elasticity (e.g. linear or rotational springs) but, despite these simplifying hypotheses, an overall analysis requires a stable multiphysics code and still remains a challenging task. Indeed, the rigid body dynamics of rotors depends on the electrostatic field and the viscous flow of the gas surrounding the MEMS. Due to the micro-scale involved, the Reynolds numbers of the flow are generally low enough to allow for the application of the steady state Stokes model. Moreover, if MEMS work at pressures where the surrounding gas can be treated as a continuum, working frequencies most often require the adoption of an incompressible fluid model.

If such an approximation is deemed acceptable, as is often the case, a pure BEM code can be applied with the considerable benefit that large relative displacements and rotations among the different substructures can be easily accounted for with minimal remeshing. The main drawback, however, is that when the problem size grows in 3D, the application of iterative solvers and accelerators (or compressors) become mandatory since BEM matrices are full. The standard multipole techniques implemented herein (see the citations in [1, 7]) allow to utilize iterative solvers in the sense that they reduce the operation count per iteration to approximately $O(N)$, to be compared with the standard $O(N^2)$ for classical approaches, where N is the problem dimension. Unfortunately, when iterative solvers are employed, spectral properties of the matrix stemming from problem discretization and preconditioning become major issues and will be discussed in the sequel.

Various approaches have been adopted in the literature for the analysis of Stokes flow via integral equations [8, 9] and some of these methodologies have been recently reviewed and compared in [4]. However most of the contributions concern 2D problems or simple 3D geometries (e.g. interacting spheres) while the main issue of MEMS is complexity; moreover few concern applications of iterative solvers and hence the conditioning of the final algebraic linear system does not play such a crucial role (see however the 2D cases analyzed in [1, 3] and the wavelet condensation put forward in [11]). The approaches available fall essentially in two main

A. Frangi (✉)
Department of Structural and Mechanical Engineering,
Politecnico of Milan, P.za L. da Vinci 32,
20133 Milano, Italy
E-mail: attilio.frangi@polimi.it

A. Frangi
Departmant of Structural Engineering,
Politecnico of Milan, Milan, Italy
E-mail: attilio.frangi@polimi.it

A. di. Gioia
Department of Mechanics,
Ecole Polytechnique, Paris, France

categories: direct and indirect methodologies. Direct formulations generally resort to the single layer potential generating first kind integral equations, while indirect formulations employ double layer kernels *completed* with concentrated single layer sources (Completed Double Layer BIE, CDL BIE, [8, 9]).

The problem of ill-conditioning is somehow intrinsic with the direct approach, as will be described in the sequel, and this is one of the main reasons why the CDL BIE has been most widely used for the analysis of viscous flows. Unfortunately, while the latter approach performs well in the presence of spheres or sphere-like bodies, numerical tests carried out by the present author on more complex geometries have led to extremely poor convergence results. Hence, focus is here set on the original single-layer formulation.

In the following sections the underlying equations are briefly recalled, analogies with other problems are stressed and implementation details are analyzed. In Sect. 3, devoted to numerical examples, some classical benchmarks are addressed and finally two real MEMS structures are analyzed.

2 Formulation

Let us consider N rigid bodies Ω^α and denote by $\underline{u}^\alpha(\underline{x})$ the velocity of Ω^α which will be assumed to be given as data. The aim is to evaluate stresses acting on the surface S^α of Ω^α according to the theory of steady state incompressible Stokes flow. If $\underline{u}(\underline{x})$ denotes fluid velocity and $p(\underline{x})$ fluid pressure, the partial differential equations of eulerian equilibrium write:

$$\nabla p(\underline{x}) - \mu \Delta \underline{u}(\underline{x}) = \underline{0} \tag{1}$$

$$\nabla \cdot \underline{u}(\underline{x}) = 0 \tag{2}$$

$$\underline{u}(\underline{x}) = \underline{u}^\alpha(\underline{x}) \quad \text{on} \quad S^\alpha \tag{3}$$

where μ is the dynamic fluid viscosity. Equations (1)–(3) represent a Dirichlet boundary value problem which, in the context of the Stokes theory, is known as ''resistance problem'' [9]; its zero-net-flux compatibility condition is automatically satisfied thanks to the hypothesis that substructures only admit rigid body motions.

Stresses inside the fluid are defined as:

$$\underline{\underline{\sigma}} = -p\underline{\underline{\mathbb{1}}} + \mu\left(\nabla \underline{u} + \nabla^{\mathrm{T}} \underline{u}\right)$$

and surface tractions are $\underline{t} = \underline{\underline{\sigma}} \cdot \underline{n}$, where $\underline{n}(\underline{x})$ is the unit normal vector to the surface.

It is well known that the Problem (1)–(3) admits, in an orthogonal Cartesian reference frame, the following integral representation ([9]):

$$u_i^\alpha(\underline{x}) = \sum_\beta \int_{S^\beta} G_{ij}\left(\underline{x}, \underline{y}\right) t_j(\underline{y}) dS, \quad \underline{x} \in S^\alpha \tag{4}$$

$$G_{ij}\left(\underline{x}, \underline{y}\right) = \frac{1}{8\pi\mu}\left(\frac{\delta_{ij}}{r} + \frac{r_i r_j}{r^3}\right) \tag{5}$$

where $r = \|\underline{y} - \underline{x}\|$, $r_i = y_i - x_i$. The incompressibility constraint Eq. (2) is automatically included in Eq. (4), in the sense that if the velocity integral equation (i.e. Eq. (4) written for a generic $\underline{x}$ position) were employed to evaluate velocities in the fluid domain the computed velocity field would be divergence free up to numerical errors.

Some major remarks arise. Equation (4) has a non trivial kernel of dimension N consisting of functions $\underline{t}^\alpha$, $\alpha \in \{1 : N\}$ such that:

$$\underline{t}^\alpha(\underline{x}) = \begin{cases} \underline{n}(x) & \underline{x} \in S^\alpha \\ \underline{0} & \text{elsewhere} \end{cases} \tag{6}$$

This requires some sort of ''regularization'' (or filtering) which will be discussed in detail in Sect. 3. It is worth stressing that the traction field $\underline{t}(\underline{x})$ also satisfies the higher order homogeneous traction equation (see [4]):

$$\frac{1}{2} t_i(\underline{x}) = \sum_\beta n_k(\underline{x}) \int_{S^\beta} T_{ijk}(\underline{x}, \underline{y}) t_j(\underline{y}) dS, \quad \underline{x} \in S^\alpha \tag{7}$$

$$T_{ijk}(\underline{x}, \underline{y}) = \frac{3}{4\pi} \frac{1}{r^5} r_i r_j r_k \tag{8}$$

where p_∞ has been assumed to vanish. The functions $\underline{t}^\alpha(\underline{x})$ (basis vectors for the kernel of Eq. (4)) do not belong to the kernel of Eq. (7).

Equation (4) is a first kind integral equation leading to a dense linear system whose spectral condition number is a-priori expected to depend on the discretisation employed; numerical experiments presented in the following sections, however, show that the major numerical difficulties do not stem from the nature of the integral equation itself, but rather from the indeterminacy described in the previous paragraph. Remedies to this ill-conditioning are the key to a successful implementation for large scale problems.

The integral formulation Equations (4) and (5) is formally identical to the one governing the Dirichlet problem for incompressible elasticity if $\underline{u}^\alpha$ is interpreted as imposed rigid-body displacements of Ω^α. Indeed the classical Kelvin kernel for elasticity reads:

$$G_{ij}^{el}\left(\underline{x}, \underline{y}\right) = \frac{1}{16\pi\mu(1-\nu)}\left((3-4\nu)\frac{\delta_{ij}}{r} + \frac{r_i r_j}{r^3}\right) \tag{9}$$

and the two kernels G_{ij}^{el} and G_{ij} coincide for $\nu = 1/2$.

A completely analogous Dirichlet problem also arises when performing the electrostatic analysis to estimate the actuating forces on the different substructures. The electric potential is assigned on the surfaces S^α and a first kind integral equation is solved to obtain the normal component of the electric field using as kernel the standard Green kernel of potential theory. Since a fully coupled analysis of MEMS also requires these particular simulations, some results will be presented in the following Sections with the aim of comparing numerical performances.

3 Numerical implementation

As customary with BEM approaches the surface of each body Ω^α is discretized into elements. In this case 3-node triangles have been employed together with a piecewise constant interpolation for tractions. Integral equations are collocated at the centroid of every BE thus providing a sufficient set of equations. The associated algebraic linear system is solved using a GMRES routine ([2]). The number of unknown parameters is hence $3M$, with M number of elements.

As anticipated in the previous Section some regularization provisions concerning the non-trivial kernel of Eq. (4) are required. Several options are available.

The Filtering Approach (FA) has been discussed e.g. in [12] and amounts to filtering out of the Krylov base of the GMRES routine the basis vectors of the kernel. This approach is effective but gets somehow more involved in the presence of a non-diagonal right-preconditioner.

A second technique, the Augmented System Approach (ASA), can be briefly explained as follows. Let us denote by $\mathbf{G}$ the algebraic system matrix, $\mathbf{t}$ the list of unknown interpolation parameters, $\mathbf{f}$ the r.h.s. vector and $\mathbf{B}$ the collection of N columns each representing the interpolation parameters of the $\underline{t}^\alpha$ base vector of the kernel. Now let the linear system $\mathbf{Gt} = \mathbf{f}$ be augmented in the following manner (see [12, 10]):

$$\mathbf{Gt} + \gamma \mathbf{B}\mathbf{B}^T = \mathbf{f}, \quad \gamma > 0 \tag{10}$$

where γ is suitable normalizing factor. In the context of symmetric approaches it can be shown that Eq. (10) strictly enforces the additional constraint:

$$\int_{S_\alpha} \underline{t} \cdot \underline{t}^\alpha \mathrm{d}S = 0, \quad \forall \alpha \in \{1 : N\}$$

making the formulation well posed. Here the collocation approach is employed and the application of Eq. (10) does not follow a rigorous proof, since matrix $\mathbf{G}$ is only approximately symmetric. It's effectiveness is however corroborated by numerical experiments.

A third possible approach is the Fictitious Compressibility Approach (FCA). In this case the Stokes problem is simulated as an elasticity one adding a limited amount of compressibility by choosing a Poisson coefficient $\nu < \frac{1}{2}$. In the limit $\nu \to 0.5$ the original ill-conditioned formulation is recovered. This of course alters the solution of the system and needs some engineering judgment to calibrate the amount of fictitious compressibility. It generally guarantees accurate results, as evidenced in the numerical examples.

The last option proposed herein (Mixed Velocity-Traction Equation Approach, MVTEA) consists in enforcing the two integral Eqs. (4) and (7) at the same time, e.g. by collocating both equations at each element centroid with a suitable weighting factor γ:

$$u_i^\alpha(\underline{x}) - \sum_\beta \int_{S^\beta} G_{ij}\left(\underline{x}, \underline{y}\right) t_j(\underline{y}) dS + \frac{\gamma}{\mu}\left(\frac{1}{2} t_i(\underline{x}) - \sum_\beta n_k(\underline{x}) \int_{S^\beta} T_{ijk}\left(\underline{x}, \underline{y}\right) t_j(\underline{y}) \mathrm{d}S\right) \tag{11}$$

Adding the traction equation is expected to have the positive effect of automatically filtering out of the solution all the components along the kernel base vectors $\underline{t}^\alpha$ (see the remarks below Eq. (8)) This approach, according to some preliminary numerical experiments, is very promising, but a complete implementation for large scale problems is still under development and hence numerical examples will focus on the second and third options.

A second major numerical issue is the need to ameliorate the iterative solution procedure. On one hand, in order to accelerate each iteration, a classical multipole approach is utilized (details are not provided herein and can be found in [7]) for the evaluation of far-field interactions, while singular and nearly singular integrals are evaluated by means of analytical formulae, [5]. On the other hand convergence speed strongly depends on the choice of the preconditioner. A natural approach, in this context, consists in utilizing the "octree" associated with multipole techniques also in order to produce a preconditioner. Indeed the structure is partitioned in a series of non overlapping cubes of different sizes containing at most Q elements, where Q is a fixed parameter to be accurately calibrated. For each of these leaves the full matrix corresponding to the elements within that leaf is constructed. The Leaf Preconditioner (LP) consists in inverting the block diagonal matrix obtained by assembling all the sub-matrices of the leaves.

Alternatively a different approach can be employed, based on physical remarks. For process reasons MEMS structures consist of several repetitive blocks, called units. It has been experimentally observed that a robust preconditioner (Unit Preconditioner, UP) can be built by partitioning the structure according to the physical units rather than according to the octree leaves and using the full matrix associated with each unit as the diagonal block of the preconditioning matrix.

It should be recalled that the final goal of the analysis is the evaluation of the total viscous drag on the structures which can be computed during the post-processing phase starting from $\underline{t}(\underline{x})$. Since the output of interest is a global measure, it can be argued (and this conclusion is supported by experimental observation) that the relative error in the global force, with respect to the value at convergence for a given mesh, will be of the same order of the relative residual computed by the GMRES routine, i.e. the residual divided by the r.h.s. norm. The stopping criterion for the GMRES solver is hence always relatively mild.

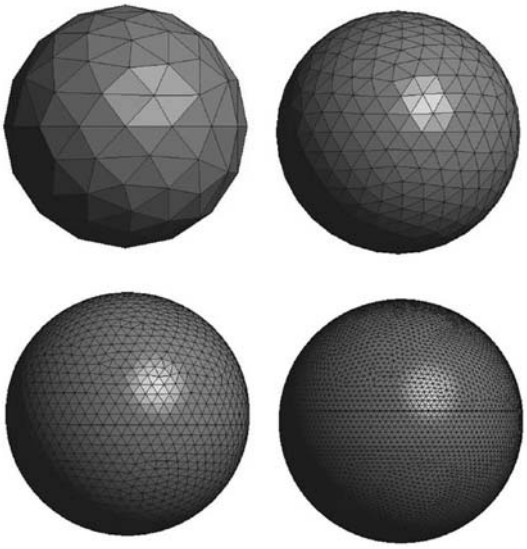

Fig. 1 Translating sphere: meshes adopted

All the examples have been run on a Windows Dell desktop, with a 2.6 GHz Intel PIV processor with 1 Gb RAM.

3.1 Translating sphere

The accuracy of the formulation is first tested against the most classical benchmark of Stokes theory. A sphere of radius R translates with velocity $\underline{u} = U\underline{e}$ in a viscous fluid, where $\underline{e}$ is the translation unit direction vector. The analytical solution is known and the global force acting on the sphere can be evaluated as: $\underline{F} = 6\pi\mu R\underline{u}$. The results of the simulation are collected in Table 1 in terms of non-dimensional force $F/(\mu RU)$ and number of iterations required to achieve a relative residual $e_{err} = 10^{-4}$.

Even if the translating sphere represents an "easy" benchmark providing well conditioned matrices with almost all the formulations employed, results collected in Table 1 put in evidence the excellent accuracy provided by the Direct Single Layer Approach, as confirmed by all the other numerical simulations presented in the following Sections.

3.2 Three-finger structure: benchmark on condition number

Before addressing more realistic examples, the simple three-finger structure depicted in Fig. 2 is analyzed, since it displays the essential geometric features of real MEMS and helps clarifying some key issues.

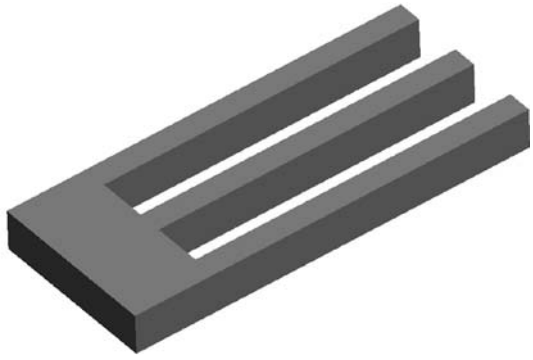

Fig. 2 Three-finger structure: geometry

Seven relatively coarse meshes are considered and analyzed employing a direct solver in order to obtain an estimate of the conditioning number c. In this case no preconditioner is applied to the system.

In Table 2 the inverse of the condition number, as evaluated by Linpack libraries, is collected for two different situations. First the case $\nu = 1/2$ (full incompressibility, Stokes case) is analyzed, with the ASA regularization as explained in the previous Section. Next the case $\nu = 0.49$ is addressed with FCA regularization. The condition number in the two cases is dramatically different, but, quite surprisingly and contrary to common belief in the literature, is almost independent of mesh refinement.

In Table 3 a parametric analysis of the inverse of the condition number has been performed as a function of the fictitious Poisson coefficient in the FCA. The mesh adopted is the third one of Table 2. Since the estimate of c^{-1} scales linearly with the difference $\left(\nu - \frac{1}{2}\right)$, it seems reasonable to conclude that the ill-conditioning of the direct single layer Stokes formulation is intrinsically linked to the incompressibility constraint.

It is however still somehow puzzling that, despite ASA regularization, the $\nu = \frac{1}{2}$ case is badly ill-conditioned, but a possible explanation on physical basis is as follows. The ASA technique filters out of the solution the base vectors of the kernel for the whole structure, but for complex geometries with slender members like those in comb-finger MEMS, several sub-structures (e.g. the fingers) numerically behave almost like separate

Table 1 Force acting on the translating sphere

Mesh	No. of elements	Force $F/(\mu RU)$	No. of iterations
1	208	18.41	10
2	800	18.72	11
3	3144	18.80	12
4	12654	18.86	16
Exact		18.84	

Table 2 Three-finger structure: inverse condition-number c^{-1}

Mesh	No. of elements	ASA	FCA ($\nu = 0.49$)
1	216	$3.32\ 10^{-5}$	$1.45\ 10^{-3}$
2	468	$2.16\ 10^{-5}$	$1.51\ 10^{-3}$
3	724	$2.06\ 10^{-5}$	$1.37\ 10^{-3}$
4	970	$2.68\ 10^{-5}$	$1.32\ 10^{-3}$
5	1214	$1.60\ 10^{-5}$	$1.31\ 10^{-3}$
6	1877	$1.84\ 10^{-5}$	$1.40\ 10^{-3}$
7	2870	$1.95\ 10^{-5}$	$1.35\ 10^{-3}$

Table 3 Three-finger structure: inverse condition number c^{-1} for mesh 3

$v = 0.3$	$v = 0.4$	$v = 0.45$	$v = 0.48$	$v = 0.49$	$v = 0.495$	$v = 0.498$	$v = 0.499$	$v = 0.4999$	$v = 0.5$
$1.15\ 10^{-2}$	$1.02\ 10^{-2}$	$6.90\ 10^{-3}$	$2.87\ 10^{-3}$	$1.37\ 10^{-3}$	$6.79\ 10^{-4}$	$2.85\ 10^{-4}$	$1.54\ 10^{-4}$	$1.37\ 10^{-5}$	$2.33\ 10^{-9}$

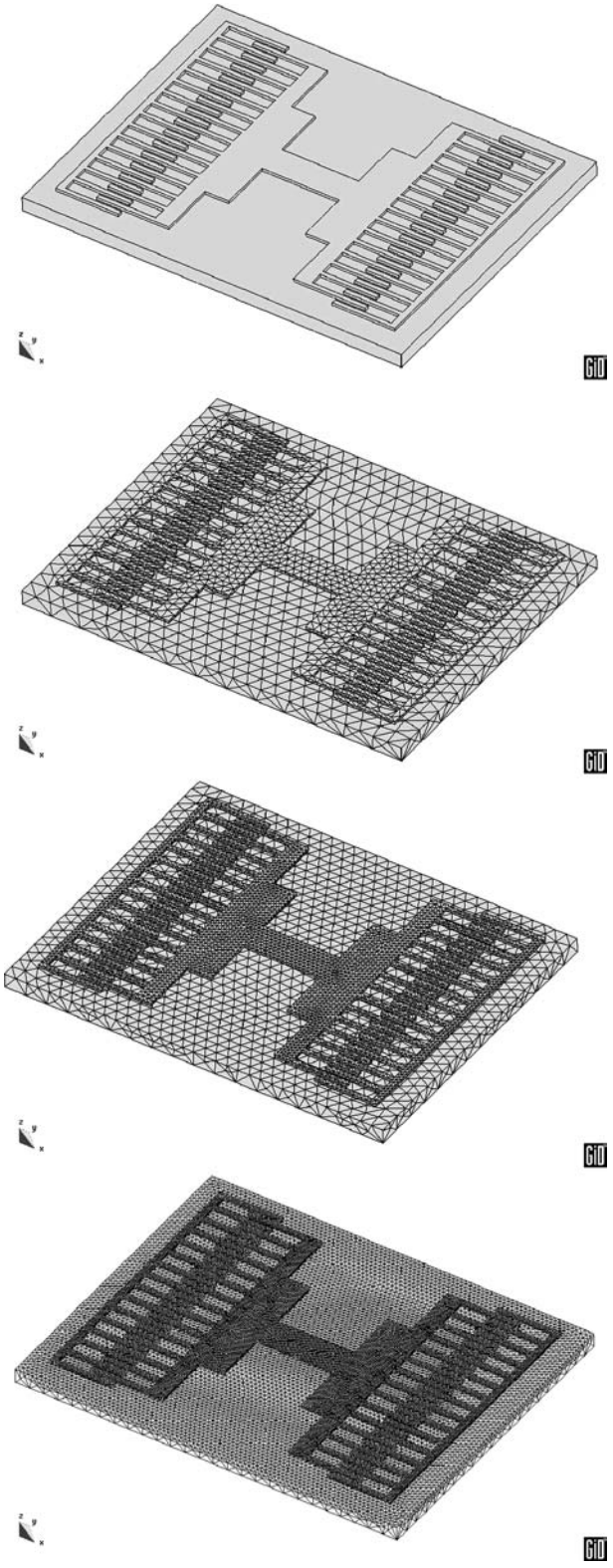

Fig. 3 Geometry and meshes for the comb-finger resonator

bodies. Since in Sect. 2 it was pointed out that the dimension of the kernel space is equal to the number of independent bodies, this represents a major source of ill-conditioning.

It is worth recalling that numerical tests have been performed also using a variational approach and reaching essentially the same conclusions.

It can be easily appreciated that the conditioning associated with the fictitious compressibility becomes comparable with that of the augmented system only for $v > 0.4999$. Since in the following Section it will be remarked that errors on the computed force are always negligible even below this threshold, the FCA regularization is generally preferred.

3.3 Comb-finger resonator

In this section the classical comb-finger resonator depicted in Figure 3 is addressed. The structure consists of a substrate, two fixed stators (one on the left and one on the right) and a rotor (in the middle) which is free to translate in a direction parallel to the fingers. A voltage difference imposed between the stators and the rotor sets the structure in resonant oscillation.

Three meshes have been tested, with 7196, 16824 and 68578 elements, respectively, preconditioning by LP, using as stopping criterion $e_{rel} = 10^{-3}$ and employing FCA regularization with Poisson coefficient $v = 0.495$. Results are collected in Table 4 where the non-dimensional force $F/(\mu UL)$, ($L = 10^{-3}$ m) is listed together with number of iterations and CPU time.

This benchmark has already been analyzed in the literature using analogous approaches: an FFT acceleration procedure in [12] and a wavelet-condensation approach in [11]. It can be mentioned that in [12] a comparison with available experimental results showed excellent correspondence.

A test has been conducted on Mesh 2 in order to analyze convergence of the force w.r.t. to the fictitious compressibility (regularization by FCA). Results are collected in Table 5.

It can be remarked that the relative difference with respect to the ASA solution ($v = \frac{1}{2}$) is $< 1\%$ for $v > 0.49$.

Table 4 Comb-finger resonator: results for the different meshes

Mesh	No. of elements	$F/(\mu UL)$	No. of iterations	CPU time (s)
1	7196	11.674	11	337
2	16824	11.824	22	1751
3	68578	11.907	63	21630
[11]		11.8		

Table 5 Comb finger resonator: convergence of force $F/(\mu UL)$

$\nu = 0.4$	$\nu = 0.45$	$\nu = 0.48$	$\nu = 0.49$	$\nu = 0.495$	$\nu = 0.498$	$\nu = 0.499$	$\nu = \frac{1}{2}$ (ASA)
11.207	11.371	11.517	11.585	11.618	11.650	11.663	11.674

Table 6 Comb-finger resonator: electrostatic simulation

Mesh	No. of elements	No. of iterations	CPU time (s)
1	7196	21	144
2	16824	22	471
3	68578	36	2836

Table 7 Parallel-plate resonator: electrostatic simulation

Mesh	No. of elements	No. of iterations	CPU time (s)
1	162529	42	5501
2	310444	43	12109
3	666376	63	33436

Several different numerical tests have been performed on different comb-finger structures and $\nu = 0.495$ has always proved to be an excellent compromise between convergence speed and accuracy.

For the sake of completeness and comparison Table 6 collects the results of an electrostatic analysis ($e_{rel} = 10^{-4}$) performed on the same structure and same meshes in order to evaluate the electrostatic actuating forces on the rotor (see Sect. 2). Once more the number of iterations increases very slowly thus denoting the good conditioning of the linear system.

3.4 Parallel plate MEMS resonator

The final example concerns a parallel plate resonator working at air pressure (see Fig. 4). The central rotor (with rectangular holes) is free to move along the direction orthogonal to the thin finger-plates, while the outer structures (stators on the right and on the left) are fixed. This is a tough benchmark since the relative motion directly "activates" the incompressibility constraint.

The structure is symmetric w.r.t. the mid plane and is highly repetitive. The analysis of the Stokes problem for the overall structure is still beyond the technical limits of the formulation and implementation produced. The electrostatic simulation, on the contrary, rapidly converges also for reasonably refined meshes. Table 7 collects results in terms of convergence obtained preconditioning by LP and stopping the analysis at a relative residuum $e_{rel} = 10^{-4}$.

A technical solution for the Stokes problem can be provided exploiting the particular layout of the resonator consisting of several identical units. First a series of different structures has been analyzed, introducing an increasing numbers of units: $1/2, 1, 3, 6$, respectively (see Fig. 5). Results are collected in Table 8, where $F/(\mu UL)$, with $L = 10^{-3}$ m, is the non-dimensional force.

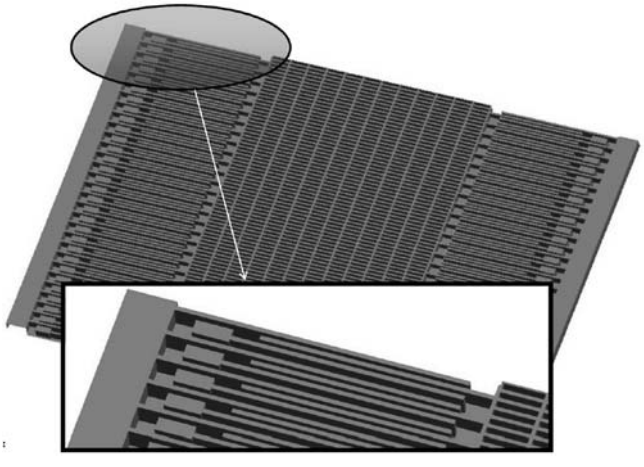

Fig. 4 Parallel-plate resonator: geometry and detail of the parallel plate fingers

Fig. 5 Parallel-plate resonator: structures with different number of units

Table 8 Parallel-plate resonator: analysis with increasing number of units

No. of units	$F/(\mu UL)$	No. of iterations	CPU time (s)
1/2	58.91	25	820
1	117.78	36	1404
3	349.85	79	5534
6	698.77	120	15020

All the analyses described in this Section have been obtained preconditioning by LP and a using stopping criterion of $e_{rel} = 10^{-2}$. The damping force acting on structure displays, as expected, a perfect linearity w.r.t. the number of units and hence focus has been eventually set on the refinement of a half unit, as depicted in Fig. 6.

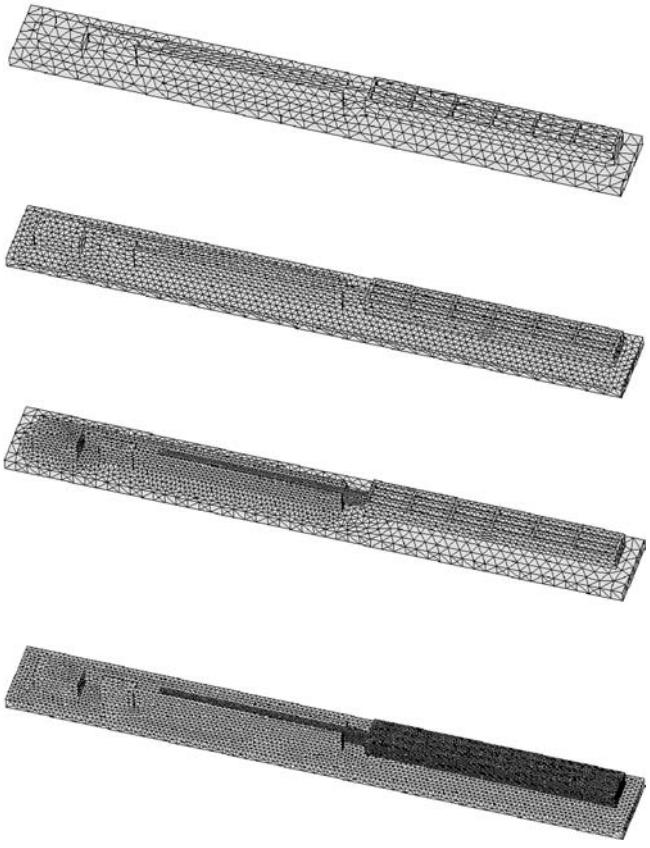

Fig. 6 Parallel-plate resonator: refinement of half-unit

Table 9 Parallel-plate resonator: refinement of half-unit

Mesh	No. of elements	$F/(\mu UL)$	No. of iterations	CPU time (s)
1	2898	42.663	13	135
2	7078	58.910	19	628
3	10484	67.961	44	1838
4	29292	69.115	68	10420

The results of the force convergence are collected in Table 9. Unfortunately, convergence is still very slow and rapidly deteriorates with mesh refinement or increasing number of units.

For the analysis of the parallel plate resonator a regularization by FCA has been used with a Poisson coefficient $v = 0.499$. The parametric variation of the Poisson coefficient yields the results collected in Table 10 for mesh 2 of Table 9. At difference from comb-finger structures, it can be appreciated that parallel plate resonators require a higher value of the Poisson coefficient which contributes in slowing the convergence of the GMRES routine.

The damping forces of Table 9 have been employed for estimating the Quality Factor (QF) of the parallel plate MEMS. The QF essentially represents the amount of dissipated energy per cycle over the maximum energy stored in the system and is widely used by industry in order to evaluate the performance of MEMS. In this case the numerical QF is 3.3, against an experimental data of 3.33, showing almost perfect agreement.

4 Conclusions

This paper collects the results of several numerical experiences conducted with the aim of evaluating damping forces on industrial MEMS. Results obtained are accurate and compare extremely well with available experimental tests. The procedure adopted applies when frequencies are relatively low (10^4–10^5 Hz) and the ambient gas can be treated as a continuum. Such conditions are met by a large number of MEMS in working conditions. More complicated models would be required to account for air compressibility (see the discussion in [12]) and high rarefaction.

This procedure is intended for use in a coupled fluid-electrostatic analysis permitting, ab-initio, the identification of parameters of reduced order models and hence represent a valid tool for the design and analysis phase of new MEMS.

Different solutions have been tested for curing the intriguing problem of ill-conditioning of the Stokes problem, with partially positive results.

Convergence speed is still not satisfactory especially when compared to results obtained in electrostatic analyses. This difficulty still hinders the application of such formulations to truly large scale problems like those addressed in electrostatic analyses and definitely deserves further attention. Two major lines of future

Table 10 Comb finger resonator: convergence of force $F/(\mu UL)$

$v = 0.4$	$v = 0.45$	$v = 0.48$	$v = 0.49$	$v = 0.495$	$v = 0.498$	$v = 0.499$	$v = 01/2$ (ASA)
11.723	18.486	29.755	39.692	48.687	56.830	58.910	58.952

development are currently under investigation: alternative formulations employing tractions integral equations (MVTEA, Sect. 3) and sophisticated preconditioners like those put forward in [10]. The former alternative has already been tested on simple cases with very encouraging results.

Acknowledgements Financial support from the EU "Design for Micro & Nano Manufacture (PATENT-DfMM)" Network of Excellence is gratefully acknowledged. The authors wish to thank J.Tausch for providing details of the comb-finger resonator geometry

References

1. Biros G, Ying L, Zorin D (2003) A fast solver for the Stokes equations with distributed forces in complex geometries. J Comput Phys 193:317–348
2. Frayssé V, Giraud L, Gratton S, Langou J, (2003) A set of GMRES routines for real and complex arithmetics on high performance computers. CERFACS technical report TR/PA/03/3
3. Gomez JE, Power H (1997) A multipole direct and indirect BEM for 2D cavity flow at low Reynolds number. Engng Analysis with Boundary Elem 19:17–31
4. Ingber MS, Mammoli AA (1999) A comparison of integral formulations for the analysis of low Reynolds number flows. Engng Analysis with Boundary Elem 23:307–315
5. Milroy JS, Hinduja S, Davey K (1997) The elastostatic three dimensional boundary element method: analytical integration for linear isoparametric triangular elements. Appl Math Modelling 21:763–782
6. Mammoli AA, Ingber MS (1999) Stokes flow around cylinders in a bounded two-dimensional domain using multipole-accelerated boundary element methods. Int J Num Meth Engng 44:897–917
7. Nishimura N (2002) Fast multipole accelerated boundary integral equation methods. Appl Mech Reviews 55:299–324
8. Power H, Wrobel L (1995) Boundary Integral Methods in Fluid Mechanics. Computational Mechanics Publications, Southampton
9. Pozrikidis C (1992) Boundary Integral and Singularity Methods for Linearized Viscous flow. Cambridge University Press, Cambridge
10. Steinbach O, Wendland WL (1998) The construction of some efficient preconditioners in the boundary element method. Adv Comput Math 9:191–216
11. Tausch J (2003) Sparse BEM for potential theory and Stokes flow using variable order wavelets. Comput Mech 32:312–318
12. Wang X (2002) FastStokes: a fast 3-D fluid simulation program for micro-electro-mechanical systems. Ph.D. Thesis, M.I.T., Boston